Journal of
Marine Science and Engineering

MDPI

Article

Acoustic Characteristics of Small Research Vessels

Miles Parsons * and Mark Meekan

Australian Institute of Marine Science, Perth, WA 6009, Australia; m.meekan@aims.gov.au
* Correspondence: m.parsons@aims.gov.au; Tel.: +61-(8)-6369-4053

Received: 20 October 2020; Accepted: 19 November 2020; Published: 27 November 2020

Abstract: Vessel noise is an acute and chronic stressor of a wide variety of marine fauna. Understanding, modelling and mitigating the impacts of this pollutant requires quantification of acoustic signatures for various vessel classes for input into propagation models and at present there is a paucity of such data for small vessels (<25 m). Our study provides this information for three small vessels (<6 m length and 30, 90 and 180 hp engines). The closest point of approach was recorded at various ranges across a flat, ≈10 m deep sandy lagoon, for multiple passes at multiple speeds (≈5, 10, 20, 30 km h^{-1}) by each vessel at Lizard Island, Great Barrier Reef, Australia. Radiated noise levels (RNLs) and environment-affected source levels (ASLs) determined by linear regression were estimated for each vessel and speed. From the slowest to fastest speeds, median RNLs ranged between 153.4 and 166.1 dB re 1 µPa m, whereas ASLs ranged from 146.7 to 160.0 dB re 1 µPa m. One-third octave band-level RNLs are provided for each vessel–speed scenario, together with their interpolated received levels with range. Our study provides data on source spectra of small vessels to assist in understanding and modelling of acoustic exposure experienced by marine fauna.

Keywords: vessel noise; radiated noise levels; monopole source levels; propagation loss

1. Introduction

Through evolutionary time, sound has become an important sensory cue for many marine taxa. The efficient transmission of sound underwater has meant that a wide variety of species have developed frequency-specific hearing sensitivity and rely on the detection of acoustic cues and subtle changes in the biophony of their local soundscape during vital life functions [1–5]. These important signals, such as the spawning calls of fishes or the sound of healthy habitat in which larvae will settle, can be masked by anthropogenic noise, disrupting natural behaviors [6–8]. Sound produced by vessels is a major element of marine anthrophony and has been recognized as a chronic stressor [9], negatively impacting communication, health and behavior of many species [4,10–15]. As human populations have increased, so too has anthrophony in oceans and inland waterways [16–21], creating what has now been termed the 'Ocean soundscape of the Anthropocene' [22].

Management strategies that aim to mitigate the impact of vessel noise on marine fauna [23–28] require information about source levels and vessel movements. Although the Automatic Information System (AIS) can be used to track passages of the majority of commercial vessels [29,30], noise is also dependent on vessel size, speed, load and power, as well as other design characteristics [24,31,32]. This requires characterization of source signatures from different types and sizes of vessels.

At present, there is little data on the noise characteristics of small (<25 m length) vessels [26,33–37]. This is important because in coastal waters, these vessels often vastly outnumber larger ships ferrying commercial cargos. The data required to accurately model the propagation of signals from small vessels are rarely reported, or typically provided as one or two measures at limited numbers of speeds [36]. For this reason, we lack data on the variability in noise among vessels of different classes (e.g., monohull, catamarans, tugs, landing craft) within this size range or even different passes of the

same vessel. This is problematic for management strategies that aim to set useful guidelines to mitigate noise for boating activities [38], particularly in shallow coastal waters, inland waterways, and coral reefs, where small vessels have the potential to significantly change the local soundscape and, due to proximity, are more likely to affect fishes, invertebrates and small marine mammals [38–42].

To address these issues, our study aimed to characterize the source spectra of three small vessels under 10 m length that are commonly used in shallow coastal marine environments. We took multiple measurements at the closest point of approach (CPA) at multiple ranges and speeds, over multiple passes, in shallow water. Source characteristics of noise can be specific to a vessel and have multiple engine-, propeller- and hull-related origins [43] and their impacts on fauna are frequency-dependent. Therefore, one-third octave levels were also calculated, and their propagation across the measured ranges investigated.

2. Materials and Methods

The International Standards Organization (ISO) protocols for the measurement of vessel radiated noise levels (RNLs) and monopole source level (MSL) focus on large vessels in deep water (see ISO 17208-1 [44] and 17208-2 [45]). The ISO criteria require a minimum water depth equal to the greater of 150 m or 1.5 times the overall ship length. For the highest standard of estimates, this comprises the deployment of three hydrophones positioned vertically at depths that result in 15°, 30°, and 45° angles from the sea surface at a CPA distance of either 100 m or one overall ship length, whichever is greater. Neither are these requirements achievable, nor is the procedure applicable, in shallow water. Indeed, meeting these requirements in Australia would require vessels to travel a significant distance offshore, which may not be appropriate for all classes of small vessels. Standards for measurements of RNL in shallow water are under development. However, we had sufficient replication of measurements to accurately estimate both RNLs and affected source levels (ASLs), in lieu of any current shallow-water ISO protocols.

2.1. Study Site

Lizard Island is a granitic island located approximately 30 km off the north Queensland coastline (14°40.88′ S, 145°27.82′ E, Figure 1). The Lizard Island group comprises four late-Permian granite islands—Lizard, Palfrey, South and Bird Islands—which, together with the surrounding fringing reef, encircle an up to 10 m-deep flat, sandy-bottomed lagoon [46]. Tidal range at Lizard Island reaches a maximum of 3 m and current speeds into the lagoon can be >30 cm s^{-1} [47,48]. Measurements were collected in the 10 m deep area of the lagoon, to the south of Lizard Island (Figure 1).

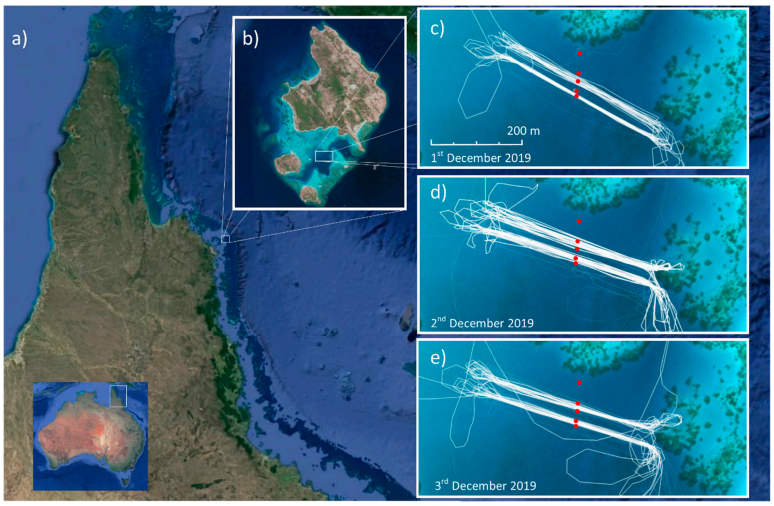

Figure 1. (**a**) Map of Australia with expansion of Cape York Peninsula, Queensland; (**b**) expansion of Lizard Island on the Great Barrier Reef; (**c**–**e**) expansions of the island lagoon with the vessel tracks from three consecutive survey days (**c**, **d**, and **e**, respectively) displayed in white and the positions of pairs of seafloor-mounted SoundTraps shown by the red dots.

2.2. Vessel Recordings

Vessel recordings were acquired using Ocean Instruments ST300 SoundTraps. These are piston-phone calibrated passive acoustic pressure sensors with a flat response of ±3 dB over the 20 Hz to 60 kHz system bandwidth, calibrated by the manufacturer using a 121 dB re 1 µPa source at 250 Hz. Divers deployed 10 ST300s on the seafloor of the lagoon, each orientated vertically, attached to the top of a star picket, and positioned approximately 50 cm above the sand. Two ST300s were deployed, 1 m apart, at each of five sites, forming a 100 m-long transect with relative spacing of 0, 10, 33.5, 52.1 and 100 m from the first site, running approximately north-south, at the northern end of the lagoon (Figure 1, red dots). All Sound Traps recorded 290 of every 300 s, at a sampling frequency of 48 kHz. Gaps between the recordings were kept to separate files into manageable sizes and minimize the potential for losing recordings due to buffering issues, and the 97% duty cycle minimized the likelihood of missing the CPA of a vessel pass. At each SoundTrap, a tight vertical line was run from the ST300 to a surface buoy where the exact GPS location was recorded with a Garmin 64SX.

Between the 1st and 3rd December 2019, three vessels (Figure 2, characteristics shown in Table 1) each conducted ten transects at speeds as close as possible to 5, 10, 20, and 30 km h^{-1} (1.4, 2.8, 5.6, and 8.3 m s^{-1}, respectively). For each speed, five transects were conducted across the southern end of the line of SoundTraps and five across the midway point (Figure 1, white lines), totaling 100 potential recordings of each vessel at each speed. Vessel transects were planned to be orthogonal to the line of SoundTraps, though in reality were not completely perpendicular to the SoundTrap transect (Figure 1). Each vessel conducted all transects over a three-hour period, with one vessel completed each day. Vessel positions were recorded using a handheld Garmin 64SX. Wind over the three days remained at Beaufort scale two or below.

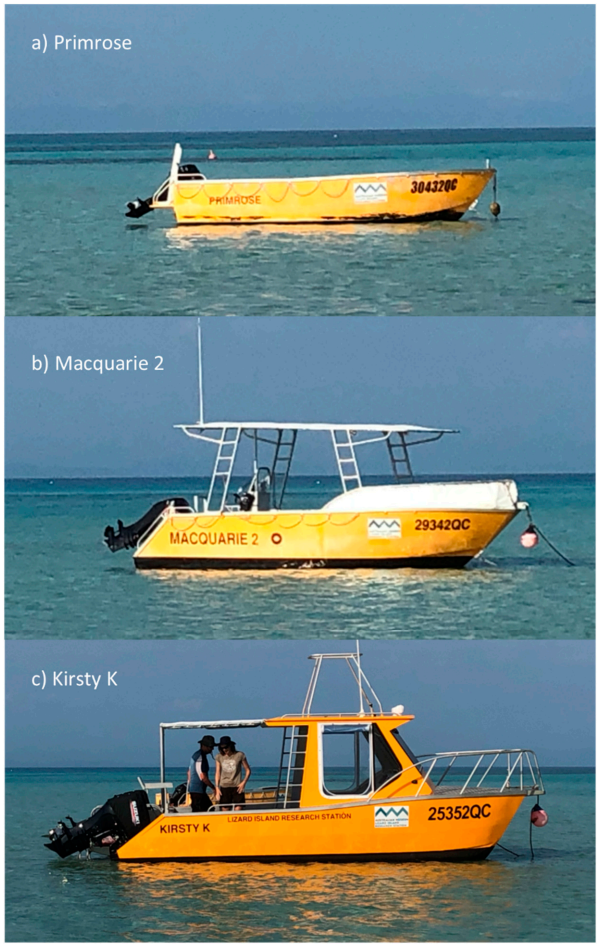

Figure 2. Photos of research vessels (**a**) *Primrose*, (**b**) *Macquarie 2* and (**c**) *Kirsty K*.

Table 1. Specifications of vessels recorded in Lizard Island lagoon.

		Primrose	Macquarie 2	Kirsty K
Vessel specifications	Length (m)	5	5.96	5.95
	Width (m)	2.1	2.4	2.6
	Draught (cm)	0.9	1.18	1.23
	Mass (kg)	360	825	1500
Propeller	No. blades	3	3	3
	Prop radius (cm)	25	32.5	32.5
	Depth below water (cm)	47	70	63
Engine	Engine	Suzuki	Suzuki	Suzuki
	Horsepower	30	90	2x90
	Fuel	Petrol (4 stroke)	Petrol (4 stroke)	Petrol (4 stroke)

2.3. Data Analysis

Data processing involved the following steps: (1) calibrating recordings, (2) selecting sections that matched the known time of each vessel pass, (3) computing mean squared pressure and power spectral density for the CPA of each transect, (4) computing RNL for each pass, and (5) least squares linear regression modelling of the recordings across all ranges to produce dipole source spectra and ASL for each vessel and speed.

The 290-s recordings were extracted, and each dataset processed with a MATLAB (version R2014, The MathWorks Inc., Nantucket, MA, USA) user interface designed for analysis of underwater passive acoustic recordings, CHORUS [49] and purpose-written functions, as well as inspected via audio and visual scrutiny of the recordings and spectrograms, respectively. Spectrograms were created in MATLAB (version R2019) using the spectrogram function with 1-s Hanning windows and 80% (=0.8) overlap. Mean squared pressure was calculated for each transect and the 1-s window that contained the maximum mean square pressure was selected to represent the received level (RL) for the vessel's CPA. Background noise levels were calculated from one-minute periods without vessel noise from each day, for each SoundTrap. RLs for each CPA were compared between pairs of SoundTraps at the same recording distance and any CPA RL with a difference greater than 5 dB were removed from analysis. CPA distance for each SoundTrap and vessel pass were determined from the known recorder positions and depth, and the GPS track of the vessel. In each case, the SoundTrap and Garmin 64SX CPA time were compared to confirm a match.

Spherical spreading losses, in the form of $20\log_{10}(\text{range})$, were back-propagated to a range of 1 m for each slant range and vessel pass to provide an estimate of RNL [50]. However, the shallow-water depth in the study area means these estimates are for comparison only as spherical spreading is unlikely reflective of the actual propagation losses (PL) at the site. Estimation of MSL is conducted by collecting measurements in the far-field and combining these with an appropriate PL model for the site, to determine the effective source level, accounting for the surface ghost, i.e., an effective RL at 1 m range [26]. However, propagation modelling, particularly in shallow water, also requires precise knowledge of the local seafloor geology, sometimes multiple meters into the substrate [37]. As this information was not available at the study site, RLs were recorded at multiple ranges from the source CPA during each transect, and broadband PLs were estimated empirically using least squares regression for a best fit curve of the RLs with range in the form of:

$$\text{SL} = C_{PL} \times \log_{10}(range) \quad (1)$$

where C_{PL} is the PL coefficient. As these RLs are a function of the propagation environment of the signal (i.e., the signal is affected by the surface reflections and interactions [51]), the value of the curve at a range of 1 m from the source may be considered an environment-affected source level (ASL).

Although hydrophones positioned directly beneath the vessel were within the acoustic near-field (for frequencies approximately ≤200 Hz) [50], these ranges reflected the type of exposure likely experienced on shallows reefs. We therefore modelled the PLs and resulting ASL estimates for each vessel and speed scenario using all data and with data from within 15 m slant range excluded, to minimize the effect of frequencies still in the near field. RNLs calculated in a shallow-water environment using spherical spreading are unlikely reflective of true PL. However, the regression-modelled PLs provide a useful proxy for acoustic propagation models, thus the broadband RLs were also back-propagated to 1 m using the average of all the regression-modelled PLs (i.e. mean C_{PL}) across all vessels and speeds (as calculated with and without measurements from the <15 m range), for comparison. Median and quartile estimates were then produced for each vessel and speed for all RNLs and ASLs. Thus, this study provides results on the RNL (percentiles are given for data including and excluding measurements taken at <15 m), the empirically measured and linear regression-modelled ASLs (with and without data from within the 15 m range) of three small vessels in shallow water.

As acoustic signals are vessel and speed specific [31,36,37,42,52], linear regression models were applied to the estimated RNL and ASLs, to investigate the relationship between source level and speed, in the form of:

$$\text{SL-SL}_{\text{ref}} = C_{v1} \times 10\log_{10}(v/v_{\text{ref}}), \quad (2)$$

where SL and SL_{ref} were the source levels at the tested and reference speeds, respectively, v and v_{ref} were the tested and reference vessel speeds, respectively, and C_{v1} was the velocity-related coefficient of the slope of the curve (Ross, 1976). If a single-coefficient, log-based regression model failed to produce a clear fit for the data, it was also investigated with a polynomial function with two coefficients:

$$\text{SL-SL}_{\text{ref}} = C_{v1} \times (v/v_{\text{ref}})^2 + C_{v2} \times (v/v_{\text{ref}}), \quad (3)$$

where C_{v2} was the second velocity-related coefficient.

Finally, received spectra for each CPA measurement were also integrated into one-third octave band levels. These band levels were interpolated across one-third octave frequency bands and range in logarithmic bins to compare the one-third octave band PL in the environment, again for each speed and vessel. One-third octave band RNLs were calculated and the frequency-dependent C_{PL} for each one-third octave band determined using linear regression of the respective band RLs recorded at various ranges, using the form of Equation (1).

3. Results

3.1. Measurements

A total of 120 transects were conducted across all three vessels and speeds (Table 2). One SoundTrap failed to provide calibrated recordings, leaving nine datasets. Of the remaining 1080 potential recordings of passes (360 for each vessel), 330, 336 and 344 CPAs were recorded of the *Primrose*, *Macquarie* and *Kirsty K*, respectively, at slant ranges between 9.0 m (almost directly below the vessel) and 98.8 m. Only two recordings were removed due to the RL of a CPA as noted by two SoundTraps at the same range differed by more than 5 dB. Average background noise levels across all sites and days were 106.8 dB re 1 µPa (max = 109.8, min = 102.3, s.d. 1.4 dB). Although the SoundTraps positioned at the greatest range were closer to the reef to the north and did contain more sounds of snapping shrimp than at the other recording sites, the mean noise at that location was <2 dB greater (108 compared with 106.2 dB re 1 µPa, respectively).

Table 2. Transect speeds conducted by each vessel (standard deviation, minimum and maximum speeds and the number of analyzed recordings shown in parentheses).

Target Speed (km h^{-1})	*Primrose* (km h^{-1})	*Macquarie* (km h^{-1})	*Kirsty K* (km h^{-1})
5	5.86 (0.12, 5.37, 6.55, 73)	6.12 (0.23, 5.63, 6.43, 88)	6.41 (0.61, 5.45, 7.66, 83)
10	10.32 (0.50, 9.73, 10.91, 79)	10.61 (1.64, 9.86, 11.61, 85)	10.62 (0.59, 9.73, 11.61, 92)
20	19.44 (0.39, 18.95, 20.28, 75)	20.63 (3.32, 18.95, 3.32, 86)	19.74 (0.52, 19.20, 20.87, 88)
30	30.23 (1.23, 28.80, 32.73, 81)	30.75 (3.30, 30.0, 33.49, 82)	30.40 (1.72, 27.17, 33.49, 86)

The approach of the vessel could be heard and observed in all recordings and spectrograms, respectively (Figure 3), though the exact CPA was more difficult to discern at the furthest ranges (>50 m) and slowest speed (5 km h^{-1}category). Lloyd's mirror interference pattern was evident on all spectrograms and propeller and engine/motor tones visible from 20 Hz through 24 000 Hz (the Nyquist frequency in this recording, Figure 3). Additionally, while not investigated fully in this study, at the close ranges (<50 m) energy in the 1–10 kHz band was typically higher in the final seconds of approach than the initial seconds of departure (Figure 3, rows a and b).

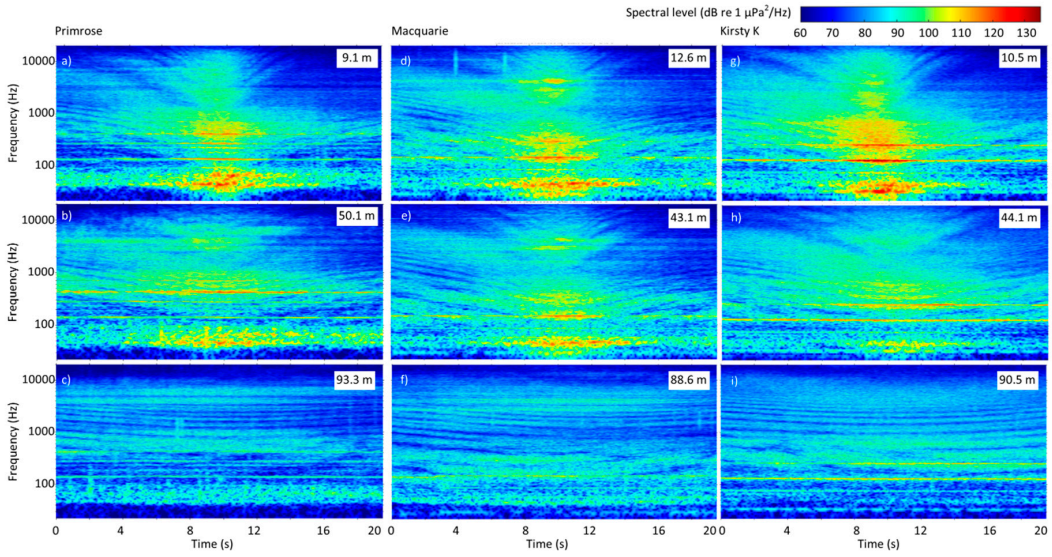

Figure 3. Spectrograms of 20 s recordings of individual passes of (**a**–**c**) *Primrose*, (**d**–**f**) *Macquarie* and (**g**–**i**) *Kirsty K* (all travelling at ≈30 km h^{-1}), as recorded almost directly (**a**,**d**,**g**) beneath the vessel (≈9 m range), (**b**,**e**,**h**) at the 25 m and (**c**,**f**,**i**) the ≈100 m ranges. CPA distance shown in top right of each spectrogram.

3.2. Received Levels with Range

In general, at a given range, RLs increased with speed for *Primrose* and *Macquarie*, though this was not as evident for the *Kirsty K* (Figure 4). Standard deviations in RLs at the same approximate speed were greatest closest to the source and standard deviations in RLs at the same range were greatest at the slowest speed category (Supplementary information). Regression models of PL varied between vessels and speeds and correlation with the recorded data was greater for transects conducted at 20 and 30 km h^{-1} than 5 and 10 km h^{-1} (Table 3). This variation was still evident when the recordings at the closest (<15 m) ranges were removed, though less so than when analyzing the full datasets. The average PL for individual datasets (vessels and speeds) for recordings across all ranges was $17.9\log_{10}(range)$, becoming $16.0\log_{10}(range)$ when data from <15 m were excluded. Standard deviation of all modelled losses decreased from 3.1 to 2.3 when removing the data taken at the <15 m range (Table 3). Percentiles of RNLs (with and without data from the <15 m range) and ASLs (using average

PL with and without data from the <15 m range) all increased with increasing engine size and speed, except the *Kirsty K* between 10 and 20 km $h^{-1}$and 20 and 30 km h^{-1}.

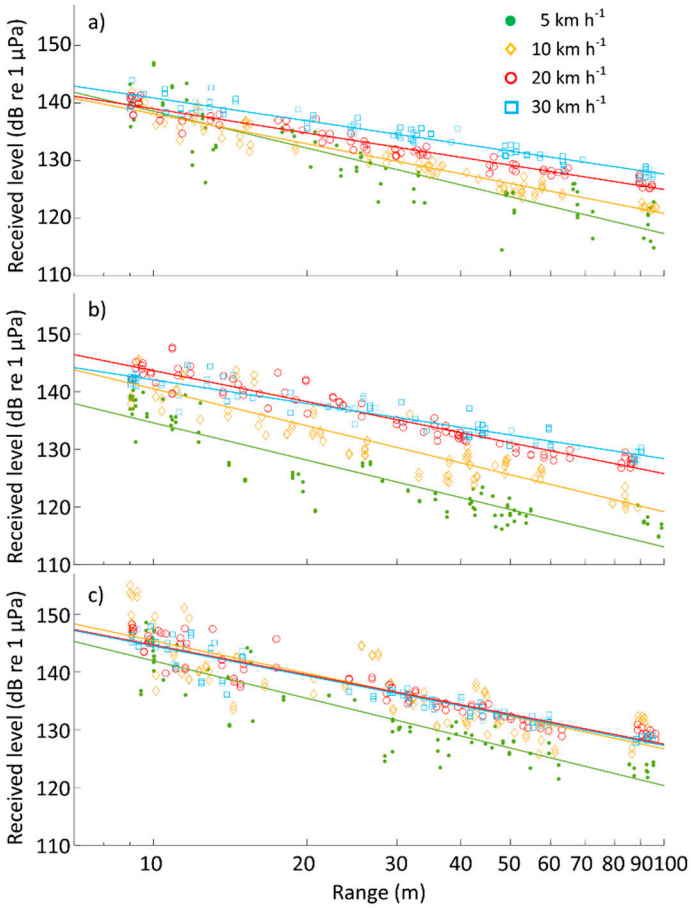

Figure 4. Received sound pressure levels from directly beneath the vessel (9 m range) to the 100 m range for (**a**) *Primrose*, (**b**) *Macquarie* and (**c**) *Kirsty K*, at speeds of 5, 10, 20 and 30 km h^{-1} (green circles, beige diamonds, red circles and blue squares, respectively).

Table 3. Propagation loss coefficients (C_{PL}) and affected source levels for individual vessels and speeds determine from Equation (1) for all ranges and for only ranges >15 m. Mean $\log_{10}$(*range*) loss values (and standard deviation) found across all regression models with all data and for ranges >15 m are also included.

		All Ranges			Excluding <15 m Range		
Vessel	**Speed**	C_{PL}	**ASL (dB re 1 µPa)**	R^2	C_{PL}	**ASL (dB re 1 µPa)**	R^2
Primrose	5	−21.2 (−23.79, −18.64)	**159.8** (156.1, 163.6)	0.79	−19.5 (−22.98, −15.96)	**156.9** (151.2, 162.7)	0.72
	10	−17.3 (−18.20, −16.33)	**155.4** (154.0, 156.8)	0.95	−16.2 (−17.44, −14.90)	**153.5** (151.4, 155.6)	0.92
	20	−14.0 (−14.72, −13.24)	**153.0** (151.9, 154.1)	0.95	−13.6 (−14.70, −12.50)	**152.4** (150.6, 154.2)	0.92
	30	−13.2 (−14.02, −12.38)	**154.1** (152.9, 155.3)	0.93	−14.5 (−15.65, −13.41)	**156.4** (154.5, 158.2)	0.92
Macquarie	5	−21.5 (−23.50, −19.52)	**156.1** (153.2, 159.0)	0.84	−12.2 (−14.95, −9.43)	**140.5** (135.9, 145.0)	0.58
	10	−21.3 (−23.31, −19.31)	**161.8** (158.8, 164.8)	0.85	−19.8 (−22.43, −17.10)	**159.2** (155.0, 163.4)	0.78
	20	−17.9 (−18.96, −16.75)	**161.5** (159.9, 163.1)	0.93	−18.3 (−19.92, −16.67)	**162.2** (159.6, 164.8)	0.90
	30	−13.7 (−14.68, −12.64)	**155.7** (154.2, 157.2)	0.90	−14.3 (−16.05, −12.57)	**156.7** (153.9, 159.6)	0.84
Kirsty K	5	−21.6 (−23.83, −19.43)	**163.6** (160.4, 166.8)	0.83	−16.7 (−20.03, −13.42)	**155.3** (149.9, 160.7)	0.67
	10	−18.7 (−21.38, −16.11)	**164.2** (160.3, 168.0)	0.69	−15.3 (−18.33, −12.21)	**158.5** (153.7, 163.2)	0.58
	20	−17.2 (−18.41, −15.97)	**161.9** (160.1, 163.7)	0.90	−15.0 (−16.62, −13.43)	**158.3** (155.7, 160.8)	0.86
	30	−17.3 (−18.40, −16.13)	**161.8** (160.1, 163.4)	0.92	−16.9 (−18.09, −15.71)	**161.2** (159.2, 163.1)	0.94
Mean C_{PL} (s.d.)		**−17.9** (3.1)			**−16.0** (2.3)		

When PL has been estimated correctly, the resulting RNL or ASL should not increase if plotted against the original range at which the measurement was taken, as can be seen for *Primrose*, using the averaged PL with data from <15 m removed (i.e., using 16.0log$_{10}$(*range*), Figure 5). This plot also illustrates the increased variation in RLs taken at ranges <15 m, compared with those at greater ranges at all speeds (Figure 5). The reduction in RL over the entire measured range would be 40 dB for spherical spreading RNLs and 32 dB for the average modelled losses at 16.0log$_{10}$(*range*). Therefore, the median ASLs, using 16.0log$_{10}$(*range*), for the *Primrose* (at 5, 10, 20 and 30 km h^{-1}, respectively) were 151.7, 153.3, 156.2, and 158.7; for the *Macquarie*, they were 146.7, 152.9, 158.2, and 159.2; and for the *Kirsty K*, they were 154.4, 159.5, 160.0, and 159.7, respectively (Table 4).

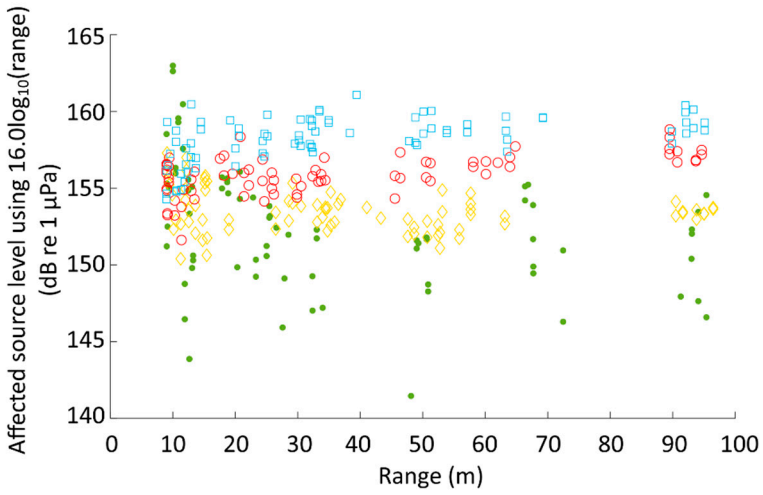

Figure 5. Affected source levels using the average linear regression-determined propagation loss across all vessels, excluding ranges below 15 m (16.0log$_{10}${*range*}) for *Primrose* at category speeds of 5, 10, 20 and 30 km h^{-1} (green dots, beige diamonds, red circles and blue square, respectively).

Table 4. Percentiles and maximum ranges of radiated noise levels and of affected source levels for the average log$_{10}$(*range*) losses across modelled losses for individual vessels and speeds using all ranges and using all ranges >15 m.

		Percentiles of Radiated Noise Level (dB re 1 µPa m)								**Percentiles of Affected Source Level (dB re 1 µPa m)**							
		All Ranges				**Excluding <15 m Range**				**Loss = 17.9log$_{10}$ (*range*)**				**Loss = 16.0log$_{10}$ (*range*)**			
Vessel	Speed	25%	**50%**	75%	Range	25%	**50%**	75%	Range	25%	**50%**	75%	Range	25%	**50%**	75%	Range
Primrose	5	155.5	**158.4**	160.2	18.8	155.6	**158.3**	159.9	14.3	152.4	**155.1**	157.4	20.2	149.3	**151.7**	153.9	14.6
	10	158.6	**159.7**	160.5	7.3	159.0	**159.9**	160.7	6.6	155.4	**156.6**	157.2	6.7	152.6	**153.3**	153.9	5.2
	20	160.3	**161.6**	163.5	10.8	161.3	**162.3**	163.9	6.9	157.6	**158.4**	159.9	8.9	155.5	**156.2**	156.9	4.7
	30	163.6	**164.8**	166.1	9.4	164.1	**165.4**	166.4	6.6	160.1	**161.3**	162.4	8.1	158.1	**158.7**	159.5	4.7
Macquarie	5	151.5	**153.4**	155.5	15.1	151.5	**153.2**	155.2	8.6	148.7	**150.5**	153.3	15.6	145.4	**146.7**	148.4	11.2
	10	158.1	**159.6**	161.2	11.4	158.0	**159.3**	161.0	10.6	154.8	**156.4**	158.0	12.2	151.4	**152.9**	154.3	10.7
	20	163.8	**164.6**	165.9	8.0	163.8	**164.5**	165.9	6.6	160.5	**161.3**	162.4	8.1	157.5	**158.2**	159.3	6.8
	30	163.9	**165.4**	166.6	12.0	164.7	**165.8**	167.1	7.9	160.0	**161.9**	163.1	10.8	158.6	**159.2**	160.4	6.4
Kirsty K	5	159.7	**161.2**	162.7	14.3	159.8	**161.0**	162.4	14.3	156.6	**158.1**	160.1	15.7	153.2	**154.4**	155.4	15.3
	10	162.9	**165.3**	169.0	16.2	163.5	**165.5**	169.7	11.9	159.7	**162.1**	166.0	17.1	157.1	**159.5**	162.7	13.3
	20	165.1	**166.0**	167.1	9.7	165.5	**166.3**	167.2	6.6	161.8	**163.0**	164.1	9.8	159.1	**160.0**	160.9	7.9
	30	165.2	**166.1**	167.1	9.6	165.7	**166.2**	167.1	4.5	162.0	**162.9**	163.6	9.5	158.9	**159.7**	160.2	3.4

3.3. One-Third Octave Band Levels

The interpolated one-third octave band levels received across the different slant ranges illustrate the interference pattern with frequency and range (Figure 6). In all three vessels, the higher frequencies increased with increasing speed, shown by the one-third octave band levels and RNLs for each vessel (Figures 6 and 7).

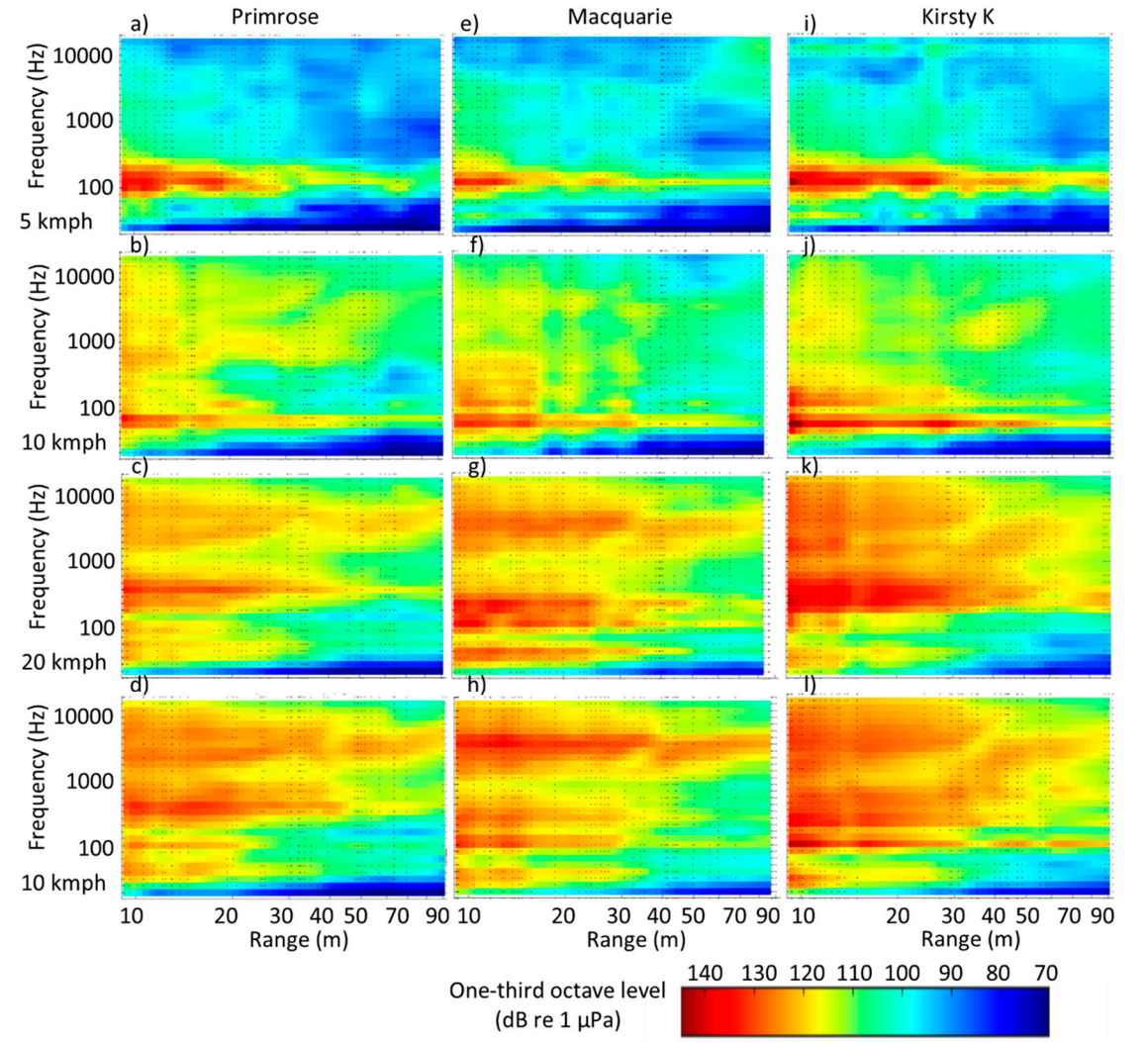

Figure 6. Interpolated (in log frequency and log range bins) one-third octave band received levels with range for each vessel (**a**–**d**, *Primrose*; **e**–**h**, *Macquarie*; **i**–**l**, *Kirsty K*), at each speed. (**a**,**e**,**i**, 5 km h^{-1}; **b**,**f**,**j**, 10 km h^{-1}; **c**,**g**,**k**, 20 km h^{-1}; **d**,**h**,**l**, 30 km h^{-1}). Black dots show the ranges at which measurements were taken to highlight gaps in interpolated data.

Linear regression determined one-third octave band PLs decreased with increasing frequency (Figure 8) from between 20 and 40 at frequencies below 50 Hz, to between 10 and 25 for frequencies between 50 and 2000 Hz. Above 2000 Hz, the propagation loss coefficients split with the vessels travelling at 5 km h^{-1} that exhibited little energy at these frequencies having coefficients of <10 (Figure 8, dots at >2000 Hz) and models for vessels with greater power and faster speeds displaying higher coefficients of 5 to 15 (Figure 8, red and green lines at >2000 Hz). Applying these frequency-dependent PL coefficients to the one-third octave band RLs produced ASL estimates higher than those derived using a single frequency-independent PL coefficient (Supplementary information).

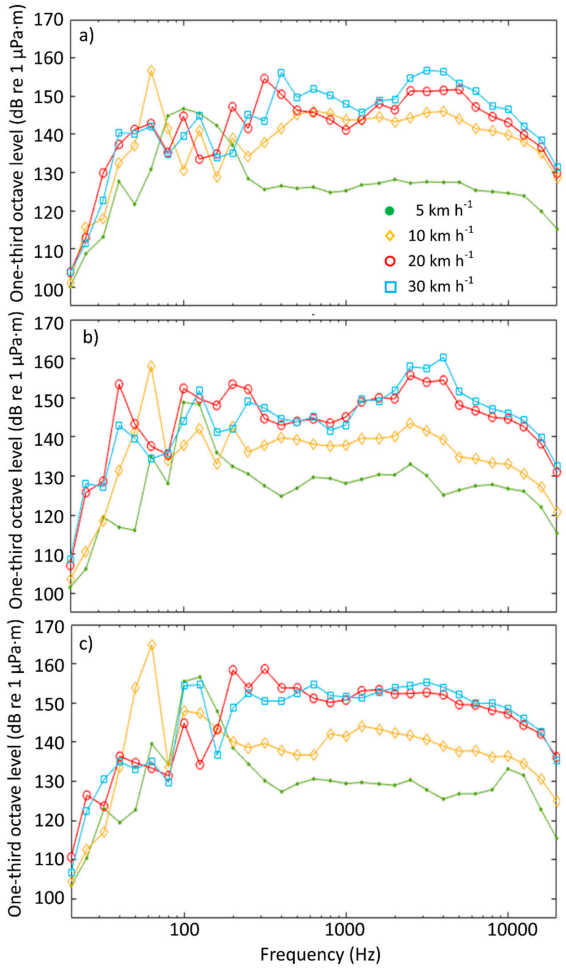

Figure 7. One-third octave radiated noise levels for (**a**) *Primrose*, (**b**) *Macquarie,* and (**c**) *Kirsty K*, at speeds of 5, 10, 20 and 30 km h^{-1} (green circles, beige diamonds, red circles and blue squares, respectively).

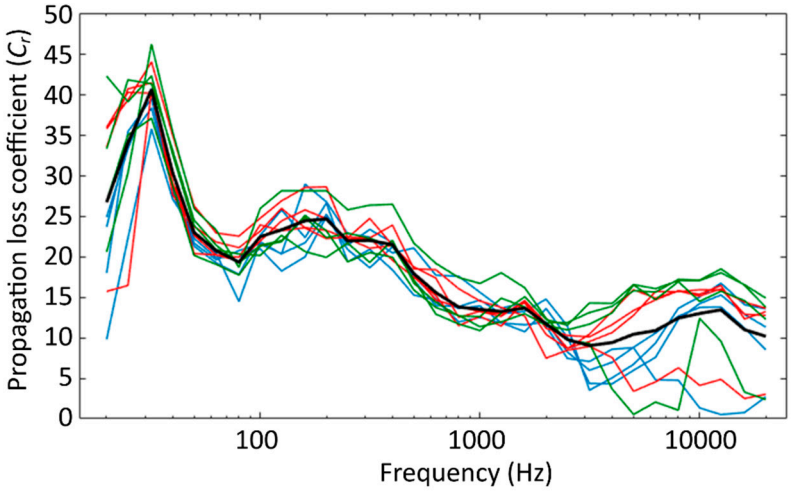

Figure 8. One-third octave band propagation loss coefficients (C_r) determined from linear regression for *Primrose*, *Macquarie* and *Kirsty K* (blue, red and green, respectively). Mean one-third octave band propagation loss coefficients across all vessels and speeds shown by the black line.

3.4. Received Levels with Speed

All three vessels displayed a general increasing trend in source level with speed, with C_{v1} values of 1.05 (s.d. = 0.09), 1.86 (0.11), and 0.68 (0.15) for the *Primrose*, *Macquarie* and *Kirsty K*, respectively (Table 5). While the *Primrose* ASLs clearly increased with each speed increase, the *Macquarie* appeared close to asymptote by 30 km h^{-1} and the *Kirsty K* appeared to reduce in source level after 20 km h^{-1} (Figure 9).

Table 5. Linear regression logistic (or polynomial for the modelled affected source levels for *Macquarie*) relationship between radiated noise levels, ASLs and averaged log_{10}(range) ASLs with speed, showing the theoretical source level at 0 km h^{-1} and remaining coefficients. Standard deviations shown in parentheses.

	Vessel	Level at 0 km h^{-1}	Coefficient C_{v1}	Coefficient C_{v2}	R^2	RMSE
RNL	*Primrose*	155.9 (0.7)	0.84 (0.11)	–	0.43	2.60
	Macquarie	151.5 (0.7)	1.55 (0.11)	–	0.68	2.87
	Kirsty K	161.6 (0.9)	0.53 (0.14)	–	0.14	3.33
ASL	*Primrose*	160.1 (0.7)	−0.78 (0.11)	–	0.43	2.44
	Macquarie	150.1 (1.2)	0.94 (0.12)	−0.50 (0.06)	0.50	2.62
	Kirsty K	165.1 (0.8)	−0.37 0.12)	–	0.09	2.97
Full data (17.9 loss)	*Primrose*	152.9 (0.6)	0.84 (0.1)	–	0.48	2.37
	Macquarie	148.4 (0.75)	1.56 (0.11)	–	0.69	2.82
	Kirsty K	158.6 (0.9)	0.53 (0.14)	–	0.15	3.32
Range >15 m (16.0 loss)	*Primrose*	148.8 (0.55)	1.05 (0.09)	–	0.73	1.73
	Macquarie	143.5 (0.75)	1.86 (0.12)	–	0.81	2.36
	Kirsty K	154.5 (11.0)	0.68 (0.15)	–	0.27	2.86

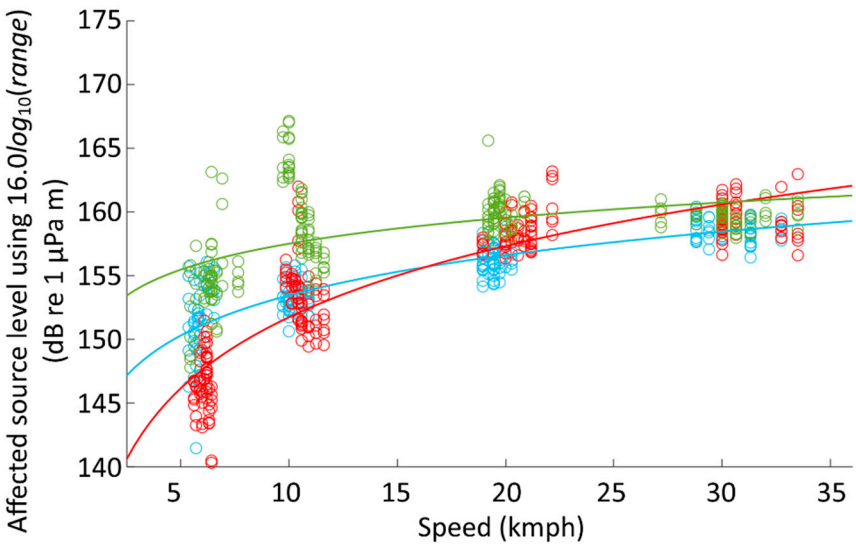

Figure 9. Relationships between affected source levels using the average linear regression-determined propagation loss across all vessels, excluding ranges below 15 m and speed for the *Primrose* (blue circles), *Macquarie* (red circles) and *Kirsty K* (green circles).

4. Discussion

Management strategies to mitigate the impacts of noise pollution by vessels in marine environments rely on an understanding of the acoustic signature of different vessel types. The variation in frequency bands in which species can detect sound means that reporting broadband RNLs or MSLs alone is insufficient information to support management decisions [36,43]. We characterized the acoustic pressure signatures for the CPA of three small (<10 m length) vessels of similar lengths, but differing

engine power, at multiple speeds. We empirically measured the propagation of their noise in shallow water (10 m depth) over the flat, sandy lagoon of a tropical granitic island, from within the near field (directly beneath the vessels at the 9 m range), out to the 100 m range. RNL and empirically modelled ASL have been determined for each speed and vessel. RNLs for small vessels, particularly those under 10 m length, are rarely reported and MSLs even less so [26,36,37,53]. Thus, the estimated RNLs, ASLs, and one-third octave band levels described here provide useful information on both shallow-water propagation of these signals and the source levels and spectra that can be applied to modelling of vessel noise.

The ISO have provided criteria for quantifying RNLs. However, the highest criteria cannot be met in Australia's shallow coastal waters. Estimation of MSLs require accurate knowledge of seafloor geomorphology (and other marine geophysical characteristics) to ensure that PL is modelled appropriately, otherwise unexpected features may arise, potentially resulting in misleading estimates [42]. Our study recorded >80 measurements at a slant ranges of between 9 and 100 m for each vessel–speed scenario to ensure PL could be estimated with confidence. RLs recorded within the closest 15 m displayed greater variation than those taken at greater ranges (Supplementary information), justifying the removal of these data from PL models on the basis that they were in the acoustic near field. This still left >50 measurements for each scenario. PL coefficients in individual vessel/speed models excluding these data ranged between 13.6 and 19.8 and produced an average coefficient of 16.0 across the 12 PL models (Table 3), approximately halfway between cylindrical and spherical spreading losses, a reasonable estimate of PL in the tested conditions [54]. As the level of required information makes the accuracy of MSL estimates difficult to assess retrospectively, we argue that measurement of RLs for multiple passes at multiple ranges to model PL through linear regression of empirical measurements was an appropriate alternative to propagation modelling for similar shallow-water cases.

Not all low-frequency energy is accounted for in this method, as indicated by the low RNLs (Figure 7) and high propagation losses (Figure 8) of one-third octave bands at frequencies below 80 Hz, as would be expected with estimates made using a dipole model. However, similar errors may also often be found in the determination of MSLs in shallow water where geomorphological information has not been accurately identified. Thus, the RNL and ASL estimates provided here are representative of the 80-20,000 Hz band. Applying linear-regression to the one-third octave band RLs to determine frequency-dependent PLs can identify where some of the low-frequency energy is missed in the RNL and ASL estimates (Figure 8, Supplementary information). However, using the vessel noise as a source can be misleading as it does not necessarily contain sufficient energy across the desired bandwidth to provide accurate PLs from linear regression. For example, vessels travelling at 5 km h^{-1} emitted relatively little sound above 2 kHz, thus the PLs appeared to be low (Figure 8, lower values of C_r at frequencies above 2 kHz). This can be alleviated by using a standardized source, such as a speaker and tone generator at the desired frequencies, though these unfortunately not available during this study. The difference between estimates of RNL (excluding data at the <15 m range) and ASL (using averaged PL models and excluding data at the <15 m range) across all vessels and speeds was 6.4 dB, while the mean difference between ASLs with and without data within the 15 m range for each scenario was -3.2 dB (s.d. = 4.9 dB, Tables 3 and 4). Additionally, the average correlation coefficient (R^2) of the individual models decreased from 0.87 to 0.80 when the data <15 m were removed (Table 3). The average difference between 25th and 75th percentiles for RNLs and averaged-loss ASLs was 2.8 dB (s.d. = 1.3, Table 4), whereas the average range was 8.8 dB (s.d. = 3.3 dB). In contrast, the average standard deviation in ASL estimates from individual speed-/vessel-specific models was 6.7 dB (Table 3). These findings show that multiple measurements of an individual vessel at the same speed can be variable and greater than the changes found by moving from a spherical spreading calculation of RNL to the linear regression-modelled ASL. Removing the near-field measurements was prudent, as this reduced the PL estimate in almost every model and the resulting estimated ASLs, albeit by less than 3 dB (Table 3).

Wladichuk et al. [36] measured multiple vessel categories, of which rigid hull inflatable boats (RHIBs) were the most similar to the vessels in this study. Broadband RNLs for these vessels were 160.9 and 167.0 dB re 1 µPa m for ≈13 and 28 km h^{-1}, respectively [36], though RHIBs were larger both in length (5.2 to 8.2 m) and engine power (150 to 700 hp) than the vessels we recorded at Lizard Island. The *Kirsty K*, the closest vessel in size and power measured here to the previously measured RHIBs [36], produced ASLs of ≈160 dB re 1 µPa m and spherical spreading RNLs of 165–166 dB re 1 µPa, at both of these speeds (Table 4). Erbe [26] and Erbe et al. [37] estimated RNLs and MSLs of various RHIBs, ranging from 7 to 9.1 m length and engine powers from 90 to 450 hp. Differences in estimated levels at any one speed, across all vessels, were found to be up to >20 dB, comparable with the variation found between the *Primrose*, *Macquarie* and *Kirsty K* (Tables 3 and 4). One vessel (6.5 m length, 90 hp) in Erbe et al. [37], produced MSLs of approximately 154, 156 and 153 dB re 1 µPa m at speeds of approximately 12, 20 and 30 km h^{-1}, respectively, in 8 m of flat water. ASL estimates of the *Macquarie*, the vessel of most similar size and power measured at Lizard Island were 152.9, 158.2 and 159.2 dB re 1 µPa m, respectively, for similar speeds (Table 4). Thus, the ASLs estimated here using PLs of $16\log_{10}(range)$ were comparable with previous measures.

Estimations of RNL and MSL typically use recordings of the CPA, or an averaged azimuth about the CPA, and assume that maximum broadband levels are received when broadside to the vessel or that there is no horizontal source directionality [37,44]. However, recorded noise levels can depend on azimuth and inclination, with some reports suggesting acoustic shielding at fore, aft or broadside, depending on the vessel design [42,55]. For example, similar to Parsons et al. [42], the recordings taken at Lizard Island displayed higher levels of acoustic energy in front of the vessel than behind, suggesting that entrained bubbles behind the vessels, generated by cavitation, have a shadowing effect after the vessel has passed. In this study, maximum levels were assumed to be broadside and directionality to be symmetrical about the centerline of the vessels, thus data from both port and starboard recordings were pooled during analysis. Any adjustment (e.g., altering power or trim) to maintain the correct speed and direction to account for wind and current can alter acoustic output of the vessel. Variations in RL recorded at Lizard Island were greatest at the slowest speed, which matched anecdotal comments from the skipper that holding the appropriate direction and line was more difficult when moving slowly. Erbe et al. [37] noted similar variability in their estimates of RNLs and MSLs of rigid-hulled inflatable boats (RHIBS) and hypothesized potential reasons for them. Acoustic output and potential shielding (e.g., by factors such as the bubble cloud and vessel hull) both contribute to the RL. Thus, changes to hull inclination and size of the cavitation vortices in the vessel wake, which occur with changes in speed or power, may be indicative of both acoustic output and dampening. Measurement of these factors could provide greater information to characterize the acoustic signature.

Ross [31] defined a relationship between vessel speed and changes in source level that Erbe [26] and then Wladichuk et al. [36] investigated for small vessels, albeit with few measures at different speeds. Broadband level increases with speed in this study comprised C_v values of 1.05, 1.86 and 0.68 for the *Primrose*, *Macquarie* and *Kirsty K*, respectively (Table 5). Wladichuk et al. [36] also observed a wide range in the same coefficient for their RHIB class (1.3 to 1.8), though they were generally higher than the three vessels studied here (Table 5). It is possible that the greater variability found at the slower speeds tested at Lizard Island (5 km h^{-1}), lack of measurements at the higher speeds (>30 km h^{-1}), yet significantly more measurements at speeds in between, can account for this difference. However, Wladichuk et al. [36] also found a much greater variation in C_v for monohulls ranging between 1.0 and 3.6, thus it is likely that the relationship between source spectra and speed is highly vessel specific.

Erbe et al. [37] noted that the decline in MSL after 20 km h^{-1} (which continued to speeds of ≈40 km h^{-1}) was likely due to reaching its 'hump' speed, when the bow-up angle was largest, producing a large trim and water resistance and therefore propeller loading. Above this speed, the vessel begins to plane, resistance and propeller loading drops, and so too does the noise level. The three vessels at Lizard Island did not display a distinct hump across the speeds measured (Figure 9). However, the asymptotic nature of the *Macquarie* and *Kirsty K* RNL and ASL curves with speed suggest

that this could have occurred between 20 and 30 km h^{-1} or about to occur with increasing speed. If measures at Lizard Island had extended to the maximum speeds of each vessel, such a relationship might have been observed. At planing speeds, Erbe et al. [37] also found that variation in RLs increased with speed, attributing this to the additional sound of vessel slap on the water for some measurements, highlighting that multiple measures are required, even for an individual speed.

At the slower speeds tested at Lizard Island, almost all energy in all three vessels occurred below 200 Hz, increasing up to 10 kHz at the faster speeds (Figure 7). Energy at all frequencies was detected at the furthest ranges for the highest vessel speeds (Figure 6). Ideally, for the same speed and vessel, the interpolated measurements of one-third octave levels would represent the similar Lloyd's mirror pattern seen in the spectrograms of the individual recordings as the vessel approaches and passes the hydrophone. This pattern can be seen to varying degrees in all scenarios in Figure 6. However, these patterns are blurred by the interpolation across range and the integration of the spectra into one-third octave bands, which blurs the narrowband energy. These frequencies were all within the hearing sensitivity range of most fishes and overlapped with those of many cetaceans [22], with the majority of energy at the most sensitive frequencies and main communication band of most fishes [56–60]. Although several studies have been conducted on the impacts of noise from such vessels on the ecology of fishes and invertebrates in recent years [61–64], and specific ways to mitigate these impacts in shallow water are being investigated [38,42], there remains a knowledge gap in this area.

Together with previous studies, the data from the *Primrose*, *Macquarie* and *Kirsty K* highlight that to fully understand a vessel's acoustic signature requires taking multiple measurements at multiple speeds and that within a given vessel class, large differences can be observed between vessels. Additional measures (e.g., data on vessel inclination, wake and size or vortices behind the vessel) may help assess the noise signature and understand differences between vessels and speeds. For appropriate modelling to be conducted with a view to mitigating the impact of noise from small vessels, a meta-analysis of all reported data is required.

Supplementary Materials: The following are available online at http://www.mdpi.com/2077-1312/8/12/970/s1, Table S1: Standard deviation in RNL estimates within shown range brackets for the various vessels and speeds, Table S2: Percentiles and maximum ranges of affected source levels calculated using propagation loss coefficients derived from linear regression of one-third octave band received levels at multiple ranges

Author Contributions: Conceptualization, M.P.; methodology, M.P. and M.M.; formal analysis, M.P.; writing—original draft preparation, M.P.; writing—review and editing, M.P. and M.M.; visualization, M.P. and M.M..; funding acquisition, M.M. All authors have read and agreed to the published version of the manuscript.

Funding: This work was undertaken for the Marine Biodiversity Hub, a collaborative partnership supported through funding from the Australian Government's National Environmental Science Program.

Acknowledgments: The authors would like to thank Drs. Mark McCormick and Jen Kelley, and the Lizard Island Research Station for logistical support and assistance during data collection. The authors would also like to thank three reviewers for the time to consider the manuscript and for their valuable suggestions.

Conflicts of Interest: The authors declare no conflict of interest. The funders had no role in the design of the study; in the collection, analyses, or interpretation of data; in the writing of the manuscript, or in the decision to publish the results.

References

1. Winn, H.E. The biological significance of fish sounds. *Mar. Bioacoust.* **1964**, *2*, 213–231.
2. Au, W.W.L.; Hastings, M.C. *Principles of Marine Bioacoustics*, 2nd ed.; Springer: New York, NY, USA, 2008. [CrossRef]
3. Radford, C.A.; Stanley, J.A.; Hole, W.; Montgomery, J.C.; Jeffs, A. Localised coastal habitats have distinct underwater sound signatures. *Mar. Ecol. Prog. Ser.* **2010**, *401*, 21–29. [CrossRef]
4. Erbe, C.; Reichmuth, C.; Cunningham, K.; Lucke, K.; Dooling, R. Communication masking in marine mammals: A review and research strategy. *Mar. Pollut. Bull.* **2016**, *103*, 15–38. [CrossRef] [PubMed]
5. Simpson, S.; Meekan, M.G.; Montgomery, J.; McCauley, R.D.; Jeffs, A. Homeward Sound. *Science* **2005**, *308*, 221. [CrossRef]

6. Simpson, S.; Radford, A.; Nedelec, S.; Ferrari, M.C.O.; Chivers, D.P.; McCormick, M.I.; Meekan, M.G. Anthropogenic noise increases fish mortality by predation. *Nat. Commun.* **2016**, *7*, 10544. [CrossRef]
7. Parsons, M.J.G.; McCauley, R.D.; Mackie, M.C.; Siwabessy, P.J.; Duncan, A.J. *In situ* source levels of mulloway (*Argyrosomus japonicus*) calls. *J. Acoust. Soc. Am.* **2012**, *132*, 3559–3568. [CrossRef]
8. Stanley, J.A.; Van Parijs, S.M.; Hatch, L.T. Underwater sound from vessel traffic reduces the effective communication range in Atlantic cod and haddock. *Sci. Rep.* **2017**, *7*, 14633. [CrossRef]
9. Van der Graaf, A.J.; Ainslie, M.A.; Andre, M.; Brensing, K.; Dalen, J.; Dekeling, R.P.A.; Robinson, S.M.; Tasker, M.I.; Thomsen, F.; Werner, S. *European Marine Strategy Framework Directive-Good Environmental Status (MSFD GES): Report of the Technical Subgroup on Underwater Noise and Other Forms of Energy (JRC Scientific and Technical Report)*; TSG Noise & Milieu Ltd.: Brussels, Belgium, 2012; 75p.
10. Weilgart, L.S. The impacts of anthropogenic ocean noise on cetaceans and implications for management. *Can. J. Zool.* **2007**, *85*, 1091–1116. [CrossRef]
11. Graham, A.L.; Cooke, S.J. The effects of noise disturbance from various recreational boating activities common to inland waters on the cardiac physiology of a freshwater fish, the largemouth bass (*Micropterus salmoides*). *Aquat. Cons. Mar. Fresh. Ecosyst.* **2008**, *18*, 1315–1324. [CrossRef]
12. Williams, R.; Erbe, C.; Ashe, E.; Beerman, A.; Smith, J. Severity of killer whale behavioral responses to ship noise: A dose response study. *Mar. Poll. Bull.* **2014**, *79*, 254–260. [CrossRef]
13. Simpson, S.D.; Radford, A.N.; Holles, S.; Ferarri, M.C.O.; Chivers, D.P.; McCormick, M.I.; Meekan, M.G. Small-Boat Noise Impacts Natural Settlement Behavior of Coral Reef Fish Larvae. In *The Effects of Noise on Aquatic Life II. Advances in Experimental Medicine and Biology*; Popper, A., Hawkins, A., Eds.; Springer: New York, NY, USA, 2016; Volume 875. [CrossRef]
14. Nedelec, S.L.; Mills, S.C.; Radford, A.N.; Belade, R.; Simpson, S.D.; Nedelec, B.; Côté, I.M. Motorboat noise disrupts co-operative interspecific interactions. *Sci. Rep.* **2017**, *7*, 6987. [CrossRef] [PubMed]
15. Erbe, C.; Marley, S.; Schoeman, R.; Smith, J.N.; Trigg, L.; Embling, C.B. The effects of ship noise on marine mammals—A review. *Front. Mar. Sci.* **2019**, *6*, 606. [CrossRef]
16. Ross, D. Ship sources of ambient noise. *IEEE J. Ocean. Eng.* **2005**, *30*, 257–261. [CrossRef]
17. McDonald, M.A. Increase in deep ocean ambient noise in the Northeast Pacific west of San Nocolas Island. *J. Acoust. Soc. Am.* **2006**, *120*, 711–718. [CrossRef] [PubMed]
18. Hildebrand, J.A. Anthropogenic and natural sources of ambient noise in the ocean. *Mar. Ecol. Prog. Ser.* **2009**, *395*, 5–20. [CrossRef]
19. Frisk, G. Noiseonomics: The relationship between ambient noise levels in the sea and global economic trends. *Sci. Rep.* **2012**, *2*, 437. [CrossRef]
20. Williams, R.; Wright, A.J.; Ashe, E.; Blight, L.K.; Bruintjes, R.; Canessa, R.; Clark, C.W.; Cullis-Suzuki, S.; Dakin, D.T.; Erbe, C.; et al. Impacts of anthropogenic noise on marine life: Publication patterns, new discoveries, and future directions in research and management. *Ocean Coast. Man.* **2015**, *115*, 17–24. [CrossRef]
21. McWhinnie, L.; Smallshaw, L.; Serra-Sogas, N.; O'Hara, P.D.; Canessa, R. The grand challenges in researching marine noise pollution from vessels: A horizon scan for 2017. *Front. Mar. Sci.* **2017**, *4*, 31. [CrossRef]
22. Duarte, C.M.; Chapuis, L.; Collin, S.P.; Costa, D.P.; Devassy, R.P.; Eguiluz, V.M.; Erbe, C.; Halpern, B.S.; Harding, H.R.; Havlik, M.N.; et al. The Ocean Soundscape of the Anthropocene. *Science* **2020**. accepted.
23. Blane, J.; Jaakson, R. The impact of ecotourism boats on the St. Lawrence beluga whales. *Environ. Cons.* **1994**, *21*, 267–269. [CrossRef]
24. Erbe, C. Underwater noise of whale-watching boats and potential effects on killer whales (*Orcinus orca*), based on an acoustic impact model. *Mar. Mamm. Sci.* **2002**, *18*, 394–418. [CrossRef]
25. Erbe, C.; Williams, R.; Sandilands, D.; Ashe, E. Identifying modeled ship noise hotspots for marine mammals of Canadas' Pacific Region. *PLoS ONE* **2014**, *9*, e89820. [CrossRef] [PubMed]
26. Merchant, N.D.; Pirotta, E.; Barton, T.R.; Thompson, P.M. Monitoring ship noise to assess the impact of coastal developments on marine mammals. *Mar. Poll. Bull.* **2014**, *78*, 85–95. [CrossRef] [PubMed]
27. New, L.F.; Hall, A.J.; Harcourt, R.; Kaufman, G.; Parsons, E.C.M.; Pearson, H.C.; Cosentino, A.M.; Schick, R.S. The modelling and assessment of whale-watching impacts. *Ocean Coast. Manag.* **2015**, *115*, 10–16. [CrossRef]
28. Cominelli, S.; Devillers, R.; Yurk, H.; MacGillivray, A.O.; McWhinnie, L.; Canessa, R. Noise exposure from commercial shipping for the southern resident killer whale population. *Mar. Poll. Bull.* **2018**, *136*, 177–200. [CrossRef] [PubMed]

29. Hatch, L.; Clark, C.W.; Merrick, R.; Van Parijs, S.M.; Ponirakis, D.; Schwehr, K.; Thompson, M.; Wiley, D. Characterizing the relative contributions of large vessels to total ocean noise fields: A case study using the Gerry E. Studds Stellwagen Bank National Marine Sanctuary. *Environ. Man.* **2008**, *42*, 735–752.
30. Erbe, C.; MacGillivray, A.O.; Williams, R. Mapping cumulative noise from shipping to inform marine spatial planning. *J. Acoust. Soc. Am.* **2012**, *132*, EL423–EL428. [CrossRef]
31. Ross, D. *Mechanics of Underwater Noise*; Pergamon Press: New York, NY, USA, 1976.
32. Chion, C.; Lagrois, D.; Dupras, J. A meta-analysis to understand the variability in reported source levels of noise radiated by ships from opportunistic studies. *Front. Mar. Sci.* **2019**, *6*, 714.
33. Au, W.W.L.; Green, M. Acoustics interaction of humpback whales and whale-watching boats. *Mar. Environ. Res.* **2000**, *49*, 469–481. [CrossRef]
34. Buckstaff, K.C. Effects of watercraft noise on the acoustic behaviour of bottlenose dolphins *Tursiops truncates* in Sarasota Bay. *Fla. Mar. Mam. Sci.* **2004**, *20*, 709–725. [CrossRef]
35. Brooker, A.; Humphrey, V. Measurement of radiated underwater noise from a small research vessel in shallow water. *Ocean Eng.* **2015**, *120*, 182–189. [CrossRef]
36. Wladichuk, J.L.; Hannay, D.E.; MacGillivray, A.O.; Li, Z.; Thornton, S.J. Systematic source level measurements of whale watching vessels and other small boats. *J. Ocean. Technol.* **2019**, *14*, 110–126.
37. Erbe, C.; Liong, S.; Koessler, M.W.; Duncan, A.J.; Gourlay, T. Underwater sound of rigid-hulled inflatable boats. *J. Acoust. Soc. Am.* **2016**, *139*, EL223–EL227. [CrossRef] [PubMed]
38. McCloskey, K.P.; Chapman, K.E.; Chapuis, L.; McCormick, M.I.; Radford, A.N.; Simpson, S.D. Assessing and mitigating impacts of motorboat noise on nesting damselfish. *Environ. Poll.* **2020**, *266*, 115376. [CrossRef]
39. Marley, S.A.; Erbe, C.; Salgado-Kent, C.P.; Parsons, M.J.G.; Parnum, I.M. Spatial and Temporal Variation in the Acoustic Habitat of Bottlenose Dolphins (*Tursiops aduncus*) within a Highly Urbanized Estuary. *Front. Mar. Sci.* **2017**, *4*, 197. [CrossRef]
40. Parsons, M.J.G.; McCauley, R.D.; Mackie, M.C. Characterisation of mulloway (*Argyrosomus japonicus*) advertisement sounds. *Acoust. Aust.* **2013**, *196*, 196–201.
41. Nedelec, S.L.; Radford, A.N.; Pearl, L.; Nedelec, B.; McCormick, M.I.; Meekan, M.G.; Simpson, S.D. Motorboat noise impacts parental behaviour and offspring survival in a reef fish. *Proc. R. Soc. B.* **2017**, *284*, 20170143. [CrossRef]
42. Parsons, M.J.G.; Duncan, A.J.; Parsons, S.K.; Erbe, C. Reducing vessel noise: An example of a solar-electric passenger ferry. *J. Acoust. Soc. Am.* **2020**, *147*, 3575–3583. [CrossRef]
43. Malinowski, S.J.; Gloza, I. Underwater noise characteristics of small ships. *Acta Acust. United Acust.* **2002**, *88*, 718–721.
44. International Organization for Standardization. *Underwater Acoustics—Quantities and Procedures for Description and Measurement of Underwater Sound from Ships—Part 1: Requirements for Precision Measurements in Deep Water Used for Comparison Purposes (ISO 17208-1)*; International Organization for Standardization: Geneva, Switzerland, 2016; 20p.
45. International Organization for Standardization. *Underwater Acoustics—Quantities and Procedures for Description and Measurement of Underwater Sound from Ships—Part 2: Determination of Source Levels from Deep Water Measurements (ISO 17208-2)*; International Organization for Standardization: Geneva, Switzerland, 2019; 13p.
46. Hamylton, S.M.; Leon, J.X.; Saunders, M.I.; Woodroffe, C.D. Simulating reef response to sea-level rise at Lizard Island: A geospatial approach. *Geomorphology* **2014**, *222*, 151–161. [CrossRef]
47. Daly, M. Wave Energy and Shoreline Response on a Fringing Reef Complex, Lizard Island, Qld, Australia. Bachelor's Thesis, Env. Sci., University of New South Wales, Sydney, Australia, 2005; 105p.
48. Frith, C.; Leis, J.; Goldmand, B. Currents in the Lizard Island region of the Great Barrier Reef Lagoon and their relevance to potential movements of larvae. *Coral Reefs* **1986**, *5*, 81–92. [CrossRef]
49. Gavrilov, A.G.; Parsons, M.J.G. A Matlab toolbox for the Characterisation of Recorded Underwater Sound (CHORUS). *Acoust. Aust.* **2014**, *42*, 191–196.
50. Urick, R.J. *Principles of Underwater Sound*, 3rd ed.; McGraw Hill: New York, NY, USA, 1983.
51. De Jong, C.A.F. Characterization of ships as sources of underwater noise. In Proceedings of the NAG-DAGA 2009, Rotterdam, The Netherlands, 23–26 March 2009; pp. 271–274.
52. Veirs, S.; Veirs, V. Vessel noise measurements underwater in the Haro Strait, WA. *J. Acoust. Soc. Am.* **2006**, *120*, 3382. [CrossRef]

53. Kipple, B.; Gabriele, C. Underwater noise from skiffs to ships. In Proceedings of the Fourth Glacier Bay Science Symposium, Junea, AK, USA, 26–28 October 2004; Piatt, J.F., Gende, S.M., Eds.; U.S. Geological Survey Scientific Investigations Report 2007-5047; 2007 U.S. Geological Survey. pp. 172–175.
54. Cato, D.H. Simple methods of estimating source levels and locations of marine animal sounds. *J. Acoust. Soc. Am.* **1998**, *104*, 1667–1678. [CrossRef] [PubMed]
55. McCauley, R.D.; Cato, D.H.; Jeffrey, A.F. *A Study of Impacts of the Impacts of Vessel Noise on Humpback Whales in Hervey Bay*; Report to the Queensland Department of Environment and Heritage; Maryborough Branch: Queensland, Australia, 1996; 163p.
56. Ladich, F.; Fay, R.R. Auditory evoked potential audiometry in fish. *Rev. Fish. Biol. Fish.* **2013**, *23*, 317–364. [CrossRef] [PubMed]
57. Kasumyan, A.O. Acoustic signaling in fish. *J. Ichthyol.* **2009**, *49*, 963–1020. [CrossRef]
58. Parsons, M.J.G.; Longbottom, S.; Lewis, P.; McCauley, R.D.; Fairclough, D.V. Sound production by the West Australian dhufish (*Glaucosoma hebraicum*). *J. Acoust. Soc. Am.* **2013**, *134*, 2701–2709. [CrossRef]
59. McWilliam, J.N.; McCauley, R.D.; Erbe, C.; Parsons, M.J.G. Patterns of biophonic periodicity on coral reefs in the Great Barrier Reef. *Sci. Rep.* **2017**, *7*, 17459. [CrossRef]
60. Montgomery, J.C.; Jeffs, A.; Simpson, S.D.; Meekan, M.G.; Tindle, C. Sound as an Orientation Cue for the Pelagic Larvae of Reef Fishes and Decapod Crustaceans. *Adv. Mar. Biol.* **2006**, *51*, 143–196.
61. Radford, A.N.; Kerridge, E.; Simpson, S.D. Acoustic communication in a noisy world: Can fish compete with anthropogenic noise? *Behav. Ecol.* **2014**, *25*, 1022–1030. [CrossRef]
62. Nedelec, S.L.; Mills, S.C.; Lecchini, D.; Nedelec, B.; Simpson, S.D.; Radford, A.N. Repeated exposure to noise increases tolerance in a coral reef fish. *Environ. Pollut.* **2016**, *216*, 428–436. [CrossRef] [PubMed]
63. Putland, R.L.; Merchant, N.D.; Farcas, A.; Radford, C.A. Vessel noise cuts down communication space for vocalizing fish and marine mammals. *Glob. Chang. Biol.* **2018**, *24*, 1708–1721. [CrossRef] [PubMed]
64. Mensinger, A.F.; Putland, R.L.; Radford, C.A. The effect of motorboat sound on Australian snapper *Pagrus auratus* inside and outside a marine reserve. *Ecol. Evol.* **2018**, *8*, 6438–6448. [CrossRef] [PubMed]